Supporting information for the manuscript

Magnetic communication and reactivity of a stable homometallic cation-cation trimer of pentavalent uranyl.

Contribution from

Lucile Chatelain, Victor Mougel, Jacques Pécaut and Marinella Mazzanti*

Laboratoire de Reconnaissance Ionique et Chimie de Coordination, SCIB, UMR-E 3 CEA-UJF , INAC, CEA-Grenoble, 17 rue des Martyrs, 38054 Grenoble Cedex 09. Fax: +33 4 38 78 5090; Tel: +33 4 3878 3955; E-mail: marinella.mazzanti@cea.fr.

*Correspondence to Dr. Marinella Mazzanti

General considerations.

All manipulations were carried out under an inert argon atmosphere using Schlenk techniques and an MBraun glovebox equipped with a purifier unit. The water and oxygen level were always kept at less than 1 ppm. The solvents were purchased from Aldrich in their anhydrous form conditioned under argon and were vacuum distilled from K/benzophenone (diisopropylether, hexane, pyridine and THF) or CaH_2 (acetonitrile, DMSO). DMSO was stored over activated 3Å molecular sieves. Anhydrous O_2 gas was purchased from Fischer Scientific and further dried over P_2O_5 for 24 hours. Depleted uranium turnings were purchased from the "Société Industrielle du Combustible Nucléaire" of Annecy (France).

Static magnetic properties were measured using a Quantum Design SQUID MPMS-XL 5.0 susceptometer. Ultra-Low Field Capability ±0.05 G for the 5 T magnets. Continuous Low Temperature Control/Temperature Sweep Mode (CLTC) - Sweep rate: 0.001 - 10 K/min. Temperature range: 2K to 300K. The samples were pressed under argon into a quartz Suprasil® container which was then introduced under argon in a 5mm Suprasil-Quartz tube with a Teflon cap. The sample container was stored under argon and transferred to the SQUID chamber under an argon flux. Contribution to the magnetization from quartz container and tube were measured independently and subtracted from the total measured signal to be corrected. Diamagnetic corrections were made using Pascal's constants. Reproducibility of the magnetic measurement was checked by the independent measurement of three doubly recrystallized samples from three different synthetic batches.

Mass spectra were acquired on a LXQ-linear ion trap (Thermo Scientific, San Jose, CA,USA), equipped with an electrospray source in a pyridine/acetonitrile mixture (1:1 to 1:5) which was prepared and filtered on microporous filters in the glove-box and maintained under argon until injection in the spectrometer. Electrospray full scan spectra, in the range of *m/z* 50 –3000 amu, were obtained by infusion through fused silica tubing at $2 – 10\ \mu L\ min^{-1}$.

The solutions were analysed in positive mode. The LXQ calibration (*m/z* 50-2000) was achieved according to the standard calibration procedure from the manufacturer (mixture of caffeine/MRFA and Ultramark 1621). The LXQ calibration (*m/z* 2000-4000) was performed with ES tuning mix (Agilent). The temperature of the heated capillary of the LXQ was set to the range of 180-220 °C, the ion spray voltage was in the range of 1-3 kV with an injection time of 5-100 ms. The experimental isotopic profile was compared in each case to the theoretical one.

Elemental analyses were performed under argon by Analytische Laboratorien GMBH at Lindlar, Germany.

^{1}H NMR spectra were recorded on Varian MERCURY 400 MHz and Bruker 200 MHz and 500 MHz spectrometers. NMR chemical shifts are reported in ppm with solvent as internal reference; the signals were assigned to the corresponding protons using COSY experiements.

The starting materials $[UI_3(THF)_4]$ [1] and $[(UO_2Py_5)(KI_2Py_2)]$ [2] were prepared according to literature procedures. Dibenzo-18-crown-6 was recrystallized twice from toluene and dried under high vacuum for 7 days. The synthesis of 2-(4-Tolyl)-1,3-bis(quinolyl)malondiimine described in the literature [3] in our hands did not yield the desired compound in significant yield, but resulted in a mixture of compounds difficult to separate. We describe here a more convenient synthetic route inspired from the synthesis of β-diketiminate ligands described by Power and co-workers [4].

Synthesis of 2-(4-Tolyl)-1,3-bis(quinolyl)malondiimine (HL)

HL is light sensitive, and therefore the reaction mixture should be protected from light.

A round-bottom flask in an ice bath was charged with 8-aminoquinoline (0.919 g, 6.38 mmol), and ethanol was added up to its entire solubilisation (5 mL). Concentrated HCl (270 µL, 3.19 mmol) was added, affording an orange suspension. To this suspension a solution of 2-(4-tolyl)malondialdehyde (0.517 g (3.19 mmol) in ethanol (20 mL) was added drop-wise maintaining the flask below 0°C. The resulting red solution was stirred 16h at room temperature and then 150 mL of dichloromethane were added. The resulting solution was neutralised at 0°C with 50 mL of a $NaHCO_3$ saturated aqueous solution. The organic layer was separated, dried over Na_2SO_4 and the volatiles were removed by vacuum distillation to provide 880mg of an orange solid (2.13 mmol, 67%). ^{1}H NMR (200MHz, DMSO-d$_6$, 298K): δ=13.97 (t, 1H), 8.83 (dd, 2H); 8.58 (d, 2H); 8.39 (dd, 2H) 7.84 (dd, 2H); 7.66 (m, 2H); 7.58 (d, 2H); 7.50 (d, 2H); 7.22 (d, 2H), 2.33 (s, 3H, -CH_3).

Synthesis of potassium 2-(4-Tolyl)-1,3-bis(quinolyl)malondiiminate (LK)

To a solution of 2-(4-Tolyl)-1,3-bis(quinolyl)malondiimine (62mg, 0.15mmol, 1 equiv) in THF (2mL) was added a suspension of KH (6 mg, 0.15mmol, 1 equiv) in THF (1mL) and the resulting reaction mixture was stirred at room temperature for 12 hours. The resulting dark violet suspension was filtered out and was washed with THF (4x1mL) and dried under vacuum to yield 53.9mg of LK (0.12mmol, 80%). The residual content of THF was evaluated for each sample by NMR.

^{1}H NMR (200MHz, CD$_3$CN, 298K): δ=8.74 (s, 4H); 8.16 (d, 2H, J^3_{H-H}=8.03Hz); 7.95 (s, 2H); 7.39 (t, 4H, J^3_{H-H}=6.9Hz); 7.26 (d, 2H, J^3_{H-H}=7.5Hz); 7.02 (d, 4H, J^3_{H-H}=7.8Hz); 2.28 (s, 3H, -CH_3).

Figure S1: Proton NMR spectra at 400 MHz and 298 K of $[UO_2(L)]_3$ in D3- acetonitrile.

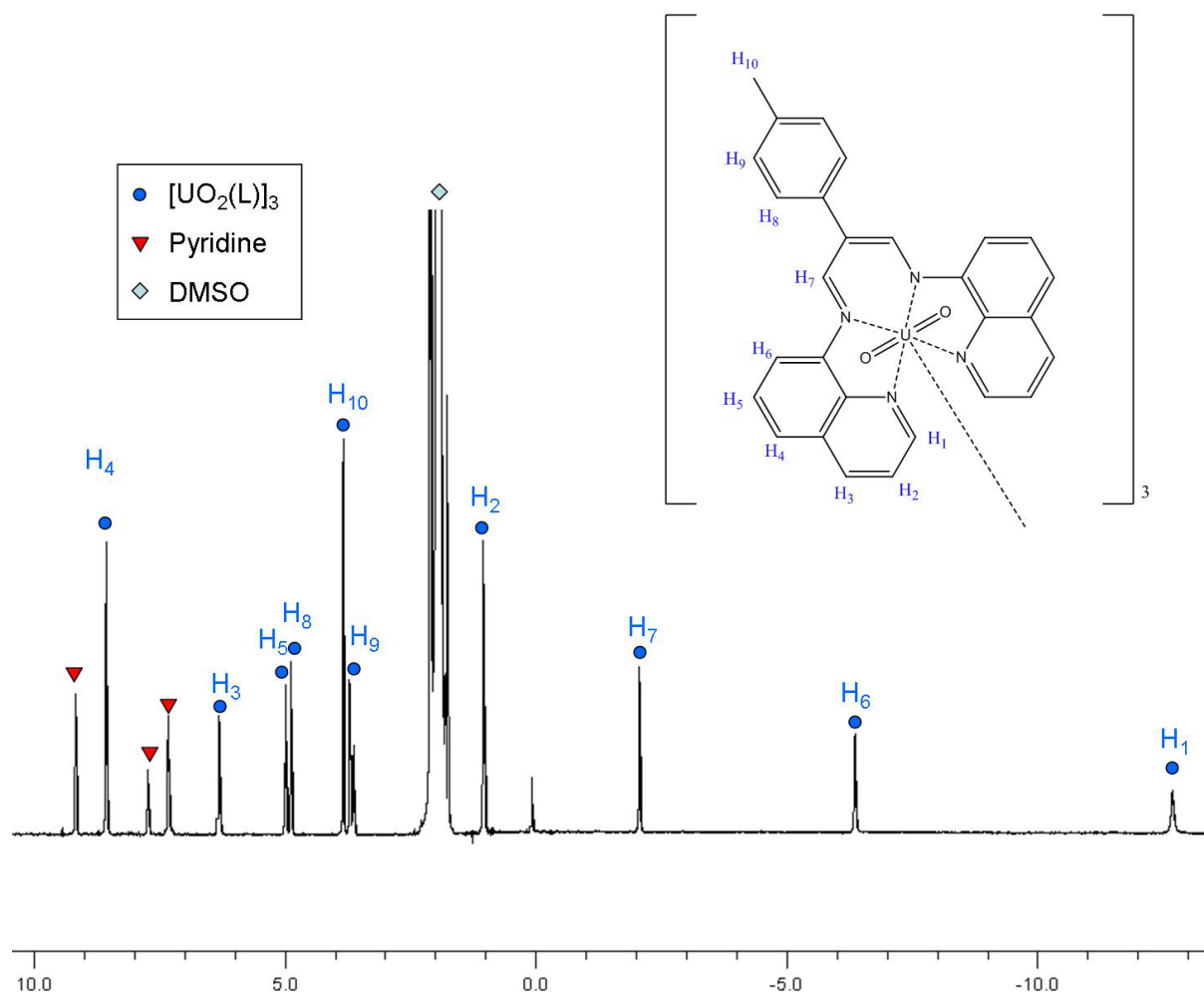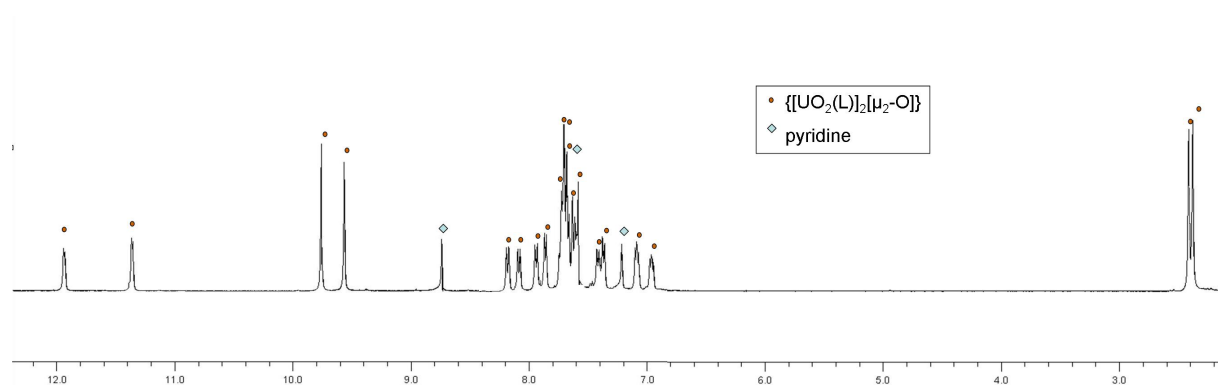**Figure S2:** Proton NMR spectra at 400 MHz and 298 K of $\{[UO_2(L)]_2[\mu_2\text{-}O]\}$ in D5-pyridine (20 mM).

Reactivity of [UO$_2$(L)]$_3$ with dichloromethane.

2.1 mg of [UO$_2$(L)]$_3$ were suspended in 1 mL of CD$_2$Cl$_2$, resulting, after 5 minutes stirring, in a clear brown solution. Proton NMR spectroscopy (see below) revealed the presence of only one set of diamagnetic signals. Slow diffusion of hexane in this solution afforded [UO$_2$(L)Cl]·CD$_2$Cl$_2$, **2**·CD$_2$Cl$_2$ as dark brown needles suitable for single crystal X-ray diffraction. The reaction can be performed on larger scale (14 mg of [UO$_2$(L)]$_3$ 3 mL of CD$_2$Cl$_2$) affording 14 mg of dark brown needles which show the same NMR and FTIR of the crystal of **2** used in X-ray diffraction.

^{1}H NMR (200MHz, CD$_2$Cl$_2$, 298K): δ=10.83 (d, 2H, J = 6.1 Hz); 9.36 (s, 2H); 8.59 (d, 2H, J = 8.5 Hz); 8.03 (m, 2H); 7.80 (m, 4H); 7.59 (d, 2H, J = 7.3 Hz); 7.43 (d, 2H, J = 7.3 Hz); 7.24 (d, 1H, J = 8.5 Hz); 2.43 (s, 3H).

Elemental analysis (%) calculated for **[UO$_2$(L)Cl]**· 0.2 CH$_2$Cl$_2$ ((C$_{28.2}$H$_{21.4}$Cl$_{1.4}$N$_4$O$_2$U 735.97 g/mol) C 46.02, H 2.93 and N 7.61, found C 45.76, H 3.18 and N 7.36

ESI-MS: 684 (UO$_2$(diket)-H$^+$)

Figure S3: Proton NMR spectra of [UO$_2$(L)]$_3$, **1** at 200 MHz and 298 K in CD$_2$Cl$_2$ after 10 minutes (1 mM) yielding the U(VI) complex [UO$_2$(L)Cl].

Figure S4: Proton NMR spectra of $[UO_2(L)]_3$, **1** at 200 MHz and 298 K in DMSO after 5 minutes (0.5 mM).
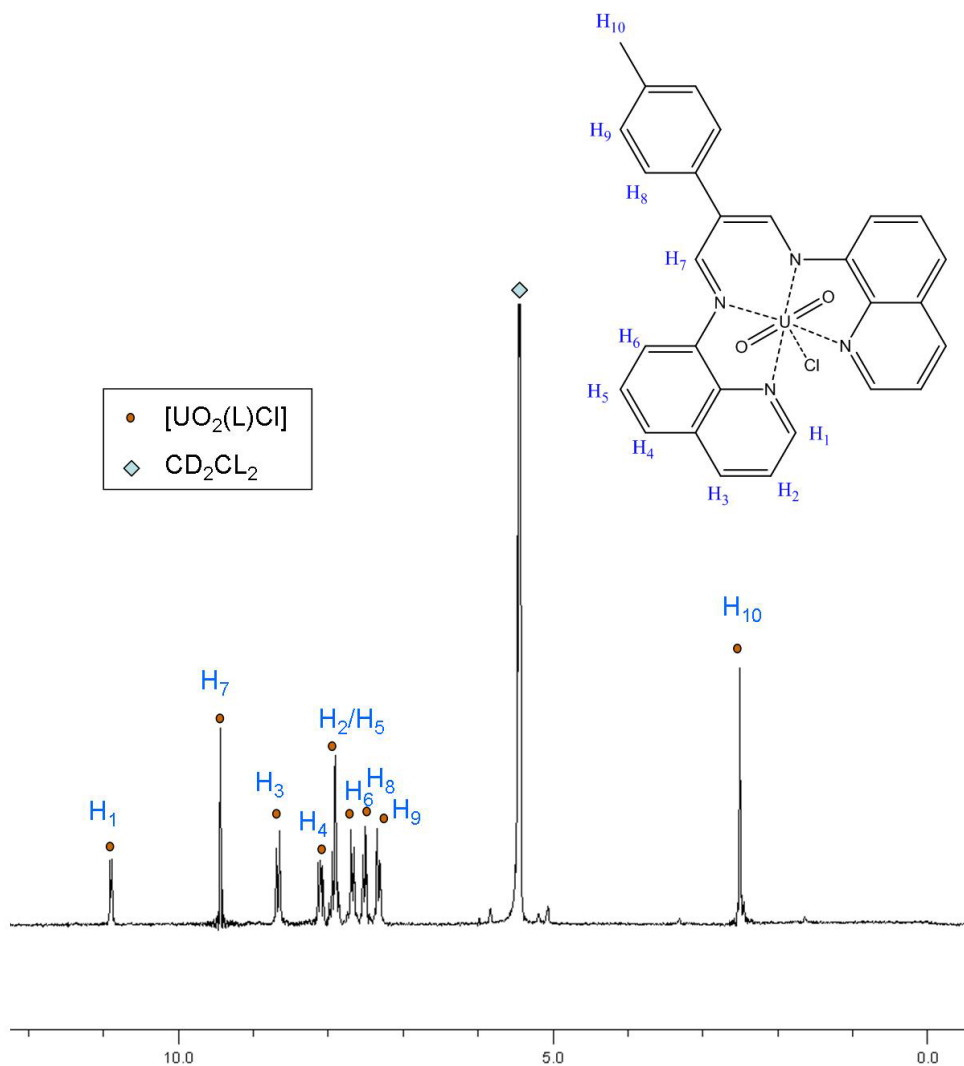
Behaviour of $[UO_2(L)]_3$ in DMSO

When $[UO_2(L)]_3$ is dissolved in DMSO, a new set of signals appears in the proton NMR spectrum which were assigned to the monomeric DMSO adduct $[UO_2(L)(DMSO)]$. This indicate that DMSO partially disrupts the trimeric assembly by competing with the uranyl oxo group for the coordination of the uranyl moiety in the equatorial plane. However, this monomer is only stable in DMSO, and when the sample in DMSO is taken to dryness and redissolved in pyridine, the original proton NMR spectra of $[UO_2(L)]_3$ is restored.
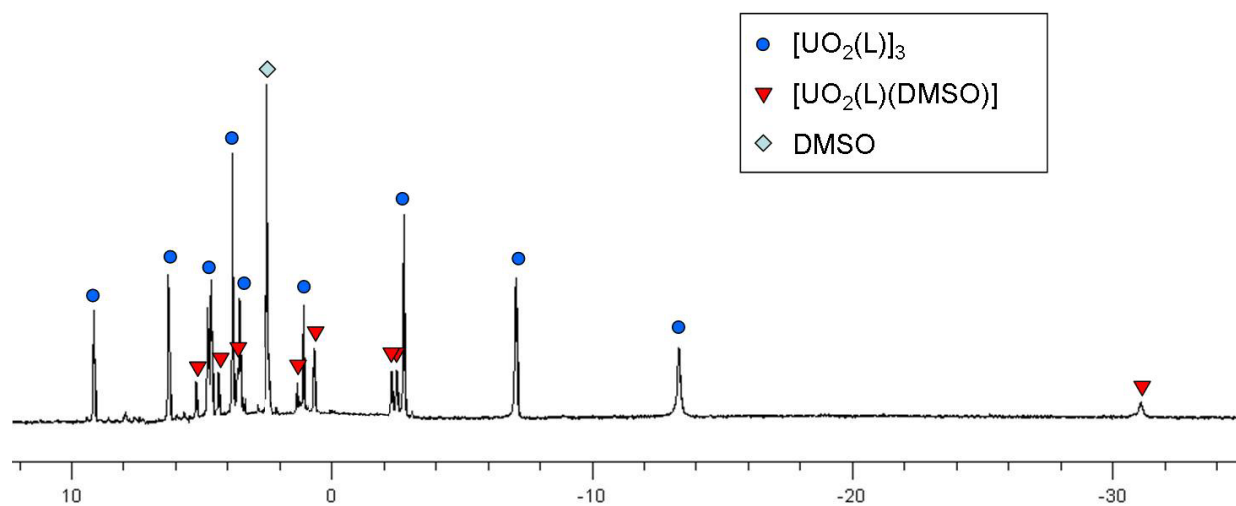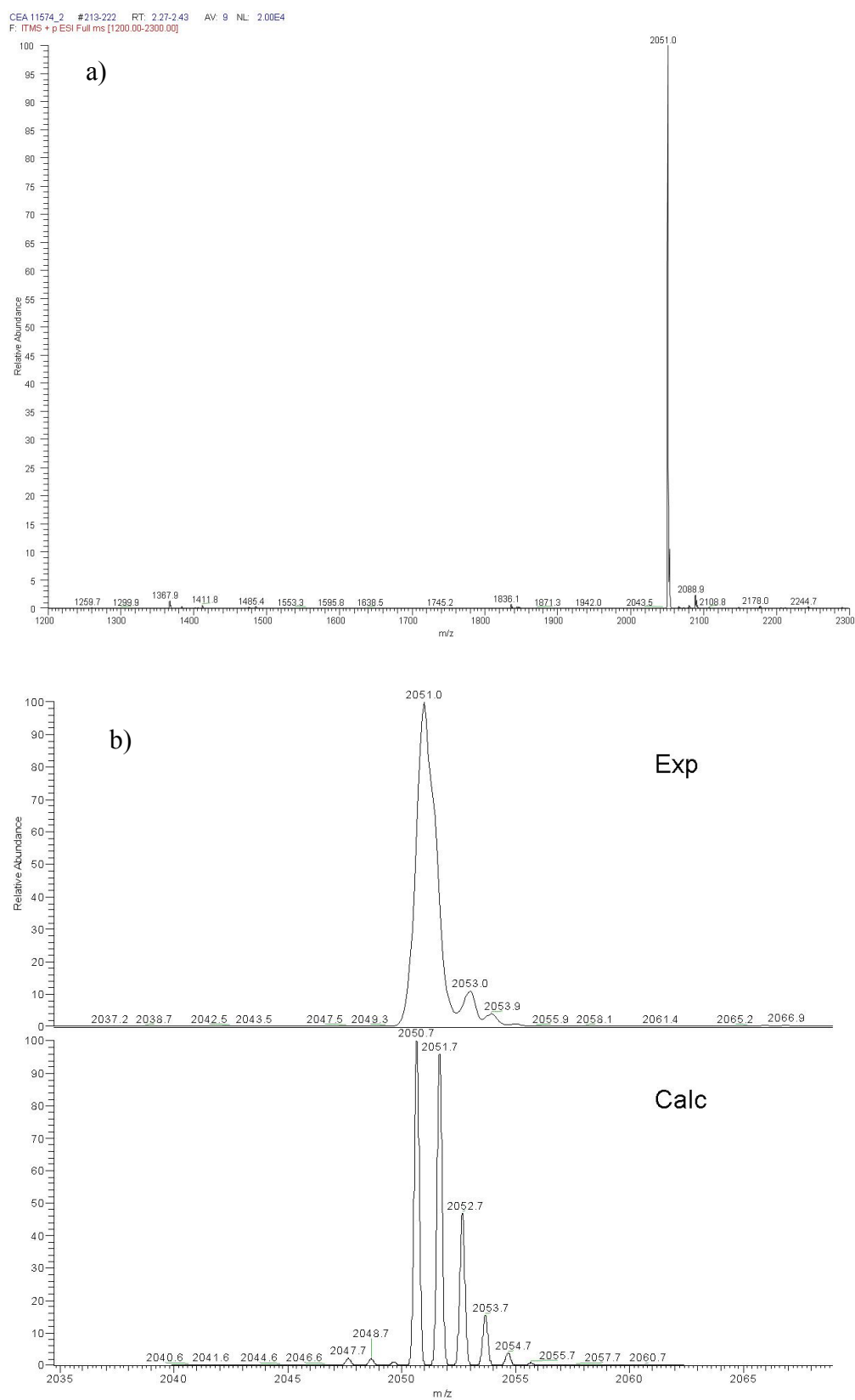
Figure S5. ESI/MS spectra of **1** in acetonitrile (a), and (b) zoom on the molecular peak compared with the theoretical isotopic profile calculated for $\{[UO_2(L)]_3-H^+\}$

X-Ray diffraction

Diffraction data were taken using a Oxford-Diffraction XCallibur S kappa geometry diffractometer (Mo-Kα radiation, graphite monochromator, λ = 0.71073 Å). To prevent evaporation of co-crystallised solvent molecules the crystals were coated with light hydrocarbon oil and the data were collected at 150 K. The cell parameters were obtained with intensities detected on three batches of 5 frames. The crystal-detector distance was 4.5 cm. The number of settings and frames has been established taking in consideration the Laue symmetry of the cell by CrysAlisPro CCD Oxford-diffraction software 336 narrow data were collected for $[UO_2(L)]_3.^iPr_2O$, $\mathbf{1}^.^iPr_2O$, 265 narrow data were collected for $\{[UO_2(L)]_2[\mu_2\text{-}O]\}$, $\mathbf{3}$ and 436 narrow data were collected for $[UO_2(L)Cl].CH_2Cl_2$, $\mathbf{2}^.CD_2Cl_2$, all with 1° increments in ω with an exposure time of 300s, 160s and 140s respectively. Unique intensities detected on all frames using the Oxford-diffraction CrysalisPro Red program were used to refine the values of the cell parameters. The substantial redundancy in data allows empirical absorption corrections to be applied using multiple measurements of equivalent reflections with the ABSPACK Oxford-diffraction program. Space groups were determined from systematic absences, and they were confirmed by the successful solution of the structure. The structures were solved by direct methods using the SHELXTL 6.14 package and for all structures all atoms, including hydrogen atoms, were found by difference Fourier syntheses. All non-hydrogen atoms were anisotropically refined whereas hydrogen atoms were fixed in ideal position.

Table S1. X-Ray crystallographic data for **[UO$_2$(L)]$_3$.^{i}Pr$_2$O, {[UO$_2$(L)]$_2$[µ$_2$-O]}** and **[UO$_2$(L)Cl]·CH$_2$Cl$_2$** .

	[UO$_2$(L)]$_3$.^{i}Pr$_2$O, 1. ^{i}Pr$_2$O	{[UO$_2$(L)]$_2$[µ$_2$-O]},2	[UO$_2$(L)Cl].CH$_2$Cl$_2$ 3. CH$_2$Cl$_2$
Formula	C90 H77 N12 O7 U3	C57.50 H44.25 N8.75 O5 U2	C29 H23 Cl3 N4 O2 U
Crystal size (mm)	0.15 x 0.05 x 0.02 mm	0.28 x 0.16 x 0.02 mm	0.20 × 0.05 × 0.03 mm
Crystal system	Monoclinic	Monoclinic	Triclinic
Space group	P 2$_1$/n	C 2/c	P -1
Volume (Å^3)	8232.7(8)	20954.7(19)	1392.11(14)
a (Å)	16.7294(13)	27.1234(13)	7.2599(4)
b (Å)	16.6323(7)	27.3660(13)	12.1368(9)
c (Å)	29.5917(11)	28.2322(16)	16.1046(8)
α (deg)	90	90	99.775(5)
β (deg)	90.954(5)	90.531(4)	90.893(4)
γ (deg)	90	90	95.133(5)
Z	4	16	2
Formula weight (g/mol)	2152.73	1413.83	803.89
Density (g/cm^3)	1.737	1.793	1.918
Absorption coefficient (mm^{-1})	5.949	6.232	6.153
F(000)	4132	10792	768
Temperature (K)	150(2)	150(2)	150(2)
Total number of reflections	53639	42381	12801
Unique reflections [R(int)]	15282 [R(int) = 0.1477]	17778 [R(int) = 0.0764]	6907 [R(int) = 0.0575]
Final R indices [I>2σ(I)]	R1 = 0.0768, wR2 = 0.1393	R1 = 0.0757, wR2 = 0.1494	R1 = 0.0759. wR2 = 0.1862
Largest diff. peak and hole (e. Å^{-3})	3.454 and -1.579 e.A^-3	3.369 and -1.593 e.A^-3	13.239 et -2.787
GOF	1.096	1.082	1.070

Figure S6: Ortep view of the coordination environment of the uranyl ion (U1) in the trimeric complex [UO$_2$(L)]$_3$.^{i}Pr$_2$O, **1**. ^{i}Pr$_2$O, with thermal ellipsoids at the 30% probability level. Hydrogen atoms were omitted for clarity.
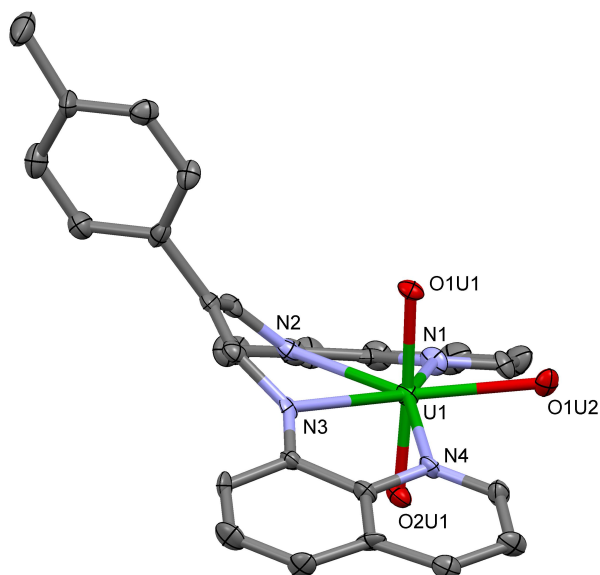

Figure S7: Side view of **2** with thermal ellipsoids at the 30% probability level. Hydrogen atoms and co-crystallised CH$_2$Cl$_2$ were omitted for clarity.
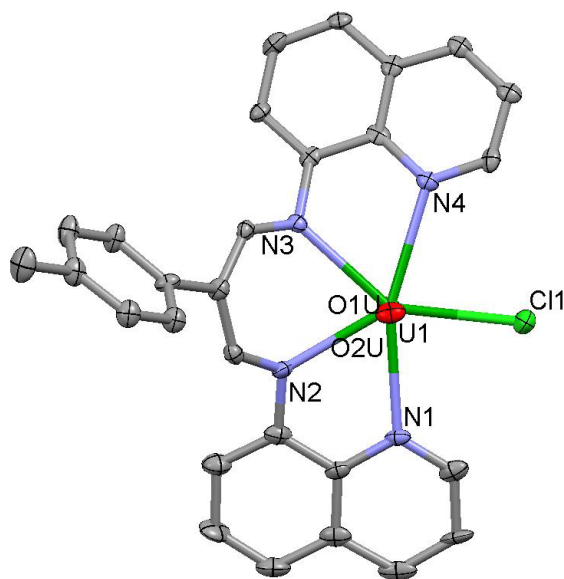
Figure S8: Plot of $1/\chi$ vs T at 5T for **1** in the range of 2-300 K. (Xdia = -1.19 × 10^{-3} emu.mol-1, $m=6.8$ mg, $M=2050$ g.mol^{-1}).
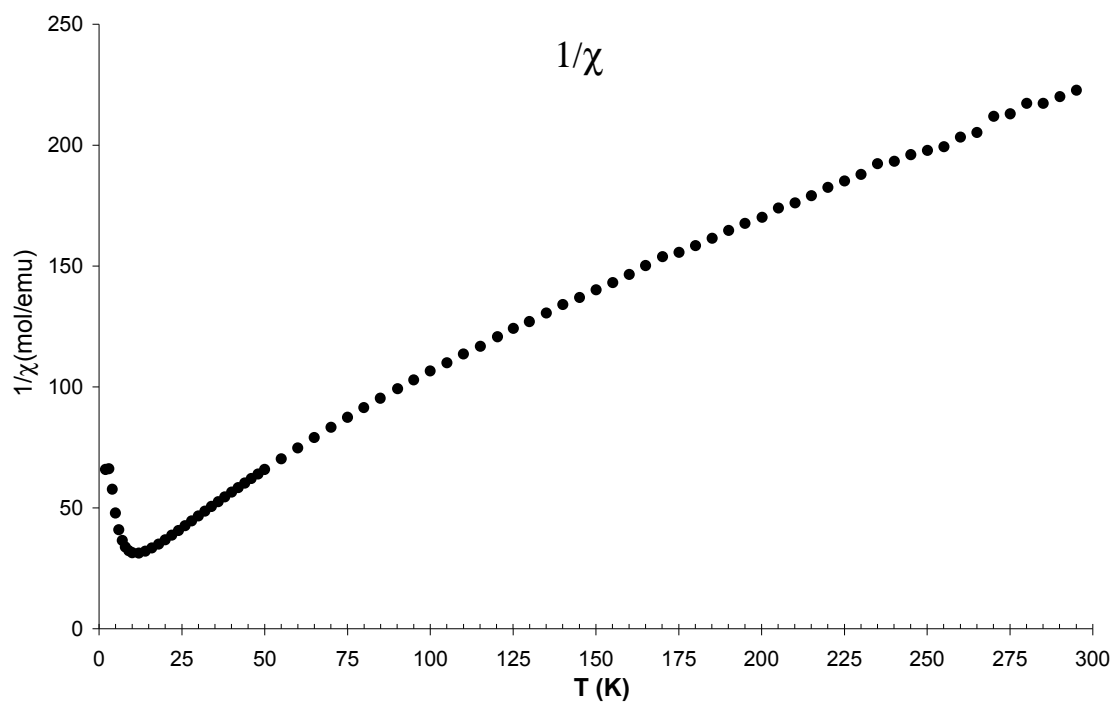

Figure S9: FTIR spectra of **1** (blue line), **2** (green line), and **3** (red line) (KBr pellets).
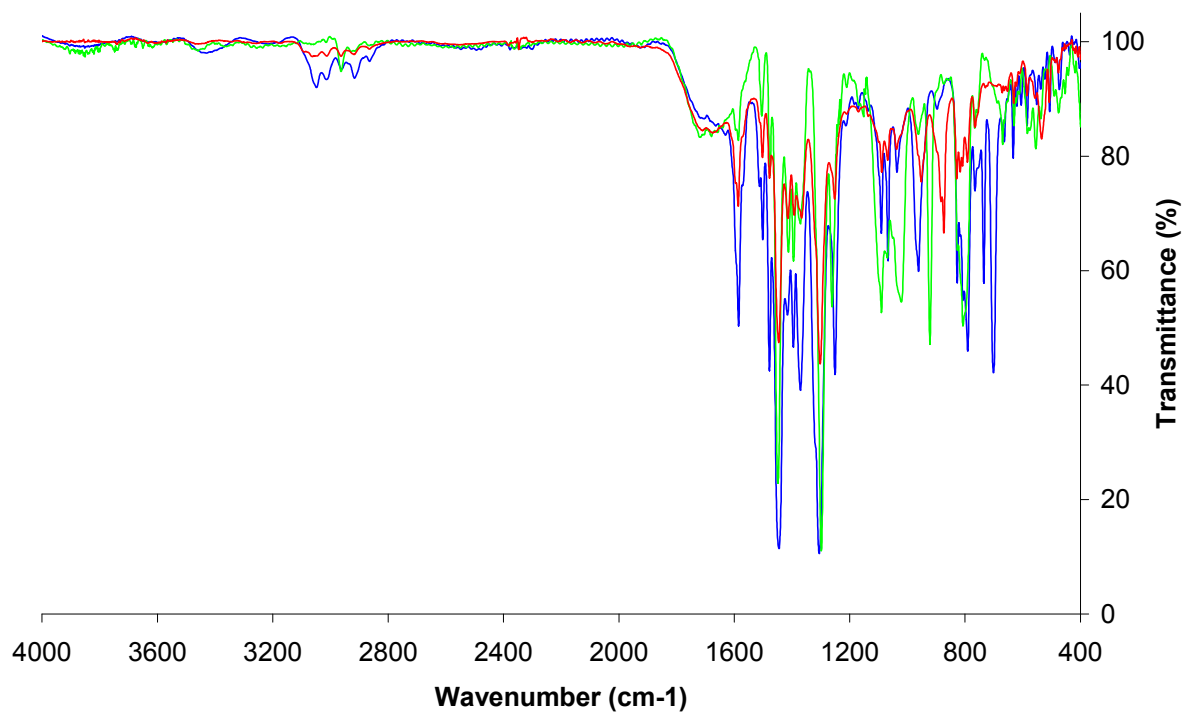
Figure S10: Detail of the 1000-400 cm^{-1} region of the FTIR spectra of **1** (blue line), **2** (green line), and **3** (red line) (KBr pellets).
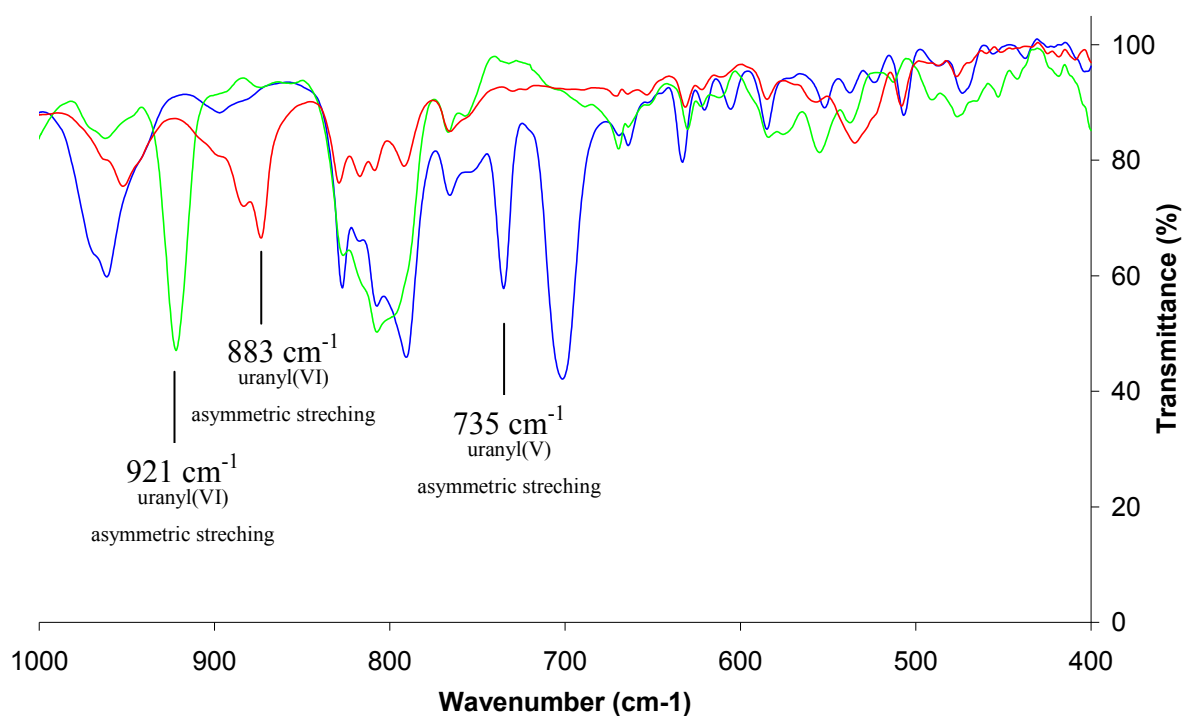

Table S2. Selected bond distances (Å) and angles (°) in complex $[UO_2(L)]_3$·$^iPr_2O$**1**·$^iPr_2O$.

Distances (Å)	
U(1)-O(2U1)	1.842(10)
U(1)-O(1U1)	1.905(10)
U(1)-O(1U3)	2.374(8)
U(1)-N(2)	2.517(10)
U(1)-N(3)	2.536(10)
U(1)-N(4)	2.605(10)
U(1)-N(1)	2.631(10)
O(1U1)-U(2)	2.371(9)
U(2)-O(2U2)	1.844(9)
U(2)-O(1U2)	1.940(8)
U(2)-N(33)	2.518(10)
U(2)-N(32)	2.537(10)
U(2)-N(34)	2.597(10)
U(2)-N(31)	2.623(9)
O(1U2)-U(3)	2.356(9)
U(3)-O(2U3)	1.820(8)
U(3)-O(1U3)	1.906(8)
U(3)-N(62)	2.524(12)
U(3)-N(63)	2.545(11)
U(3)-N(64)	2.618(10)
U(3)-N(61)	2.627(10)

Angles (°)	
O(2U1)-U(1)-O(1U1)	176.7(4)
U(1)-O(1U1)-U(2)	157.1(5)
O(2U2)-U(2)-O(1U2)	176.4(3)
U(2)-O(1U2)-U(3)	156.4(4)
O(2U3)-U(3)-O(1U3)	176.7(4)
U(3)-O(1U3)-U(1)	154.9(5)

Table S3. Selected bond distances (Å) and angles (°) in complex $\{[UO_2(L)]_2[\mu_2\text{-}O]\}$, **3**.

Distances (Å)	
U(1)-O(2U1)	1.789(11)
U(1)-O(1U1)	1.795(10)
U(1)-N(2)	2.554(12)
U(1)-N(3)	2.460(14)
U(1)-N(1)	2.649(13)
U(1)-N(4)	2.696(15)
U(1)-O(1)	2.186(13)
U(2)-O(1)	2.198(13)
U(2)-O(2U2)	1.822(10)
U(2)-O(1U2)	1.803(11)
U(2)-N(32)	2.494(13)
U(2)-N(33)	2.517(15)
U(2)-N(31)	2.585(13)
U(2)-N(34)	2.604(13)
C(91)-C(79)	3.240
C(92)-C(80)	3.535

Angles (°)	
O(2U)-U(1)-O(1U)	176.2(5)
O(2U)-U(1)-O(1U)	172.8(5)
U(1)-O(1)-U(2)	177.2(7)

**Table S4.** Selected bond distances (Å) and angles (°) in complex [UO$_2$(L)Cl].CH$_2$Cl$_2$

Distances (Å)	
U(1)-O(2U)	1.757(9)
U(1)-O(1U)	1.785(8)
U(1)-N(2)	2.467(10)
U(1)-N(3)	2.485(9)
U(1)-N(1)	2.614(9)
U(1)-N(4)	2.620(10)
U(1)-Cl(1)	2.689(3)

Angles (°)	
O(2U)-U(1)-O(1U)	178.4(4)
O(2U)-U(1)-Cl(1)	90.9(3)
O(1U)-U(1)-Cl(1)	90.1(3)

Diffusion coefficient measurement

The diffusion NMR experiments were performed using a Pulsed-Field Gradient STimulated Echo (PFGSTE) sequence, using bipolar Gradients, at 298 K and no spinning was applied to the NMR tube. [5-7]

The following BPP-LED (**B**ipolar **P**ulse **P**air – **L**ongitudinal **E**ddy-current **D**elay) pulse sequence was applied[6]:
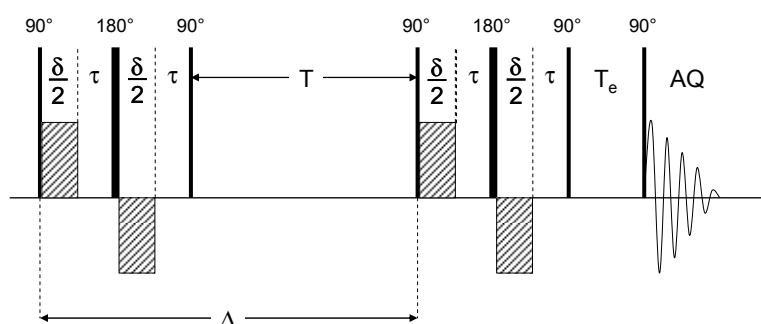
$\delta = 2$ ms. $\tau = 0.5$ ms.

The diffusion times T were optimized at 170 ms. The evolution of the pulsed-field gradient during the NMR diffusion experiments was established in 20 steps, applied linearly between 9.2 and 41.6 G.cm^{-1} for $[UO_2(L)]_3$ and between 2.7 and 33.7 G.cm^{-1} for the oxidized complex.

In the present sequence the intensity of the signal is given by the following equation: [6]

$$I(q) = I(0).\exp\left[-D.q^2\left(\Delta - \frac{\delta}{3} - \frac{\tau}{2}\right)\right] \quad \text{with } q = \gamma.\delta.g$$

and D : diffusion coefficient (m².s^{-1}), Δ: time between the two gradient pulse sequences (s), δ : bipolar gradient duration (s), τ : pulse separation delay (s), γ : magnetogyric ratio of the observed nucleus (s^{-1}.T^{-1}) and finally g : gradient strength (T.m^{-1}).

The diffusion coefficient is then the slope of the line obtained by plotting $\ln(I/I_0)$

against $q^2 \cdot \left(\Delta - \dfrac{\delta}{3} - \dfrac{\tau}{2} \right)$

Spherical hydrodynamic radius

The spherical hydrodynamic radius (called Stokes radius) of the molecule was calculated from the Stokes-Einstein equation and compared to the value obtained from the solid state structure and with a similar reference compound in the same solvent:

$$r_{sph} \left(r_{sph} = \frac{k_B \cdot T}{6\pi \cdot \eta \cdot D} \right)$$

η (Pa.s) = viscosity of the medium ; k_B (m².kg.s^{-2}.K^{-1}) = Boltzmann constant.

T : absolute temperature (K); D : diffusion coefficient (m².s^{-1})

The values of the diffusion coefficient obtained for a 0.14 mM solution of $[UO_2(L)]_3$ in pyridine were compared with those measured for the monomeric $[UO_2(L)Cl]$ complex in the same solvents and at the same temperature. The hydrodynamic radii calculated from the measured coefficient diffusion values are in good agreement with the spherical radii were evaluated from the crystal structure by considering the volume of the ellipsoid determined by the three main dimensions and calculating the radius of a sphere of the same volume.

Table 4 : Diffusion coefficient values and estimated spherical radii.

Solvent	Compound	D [m².s^{-1}]	r_{sph} [Å]$_{exp}$	r_{sph} [Å] (evaluated from crystal structure)
Pyridine η=0.879 mPa.s (298K)	$[UO_2(L)]_3$	4.906×10^{-10} $\pm$ 1.248×10^{-10}	5.1	6.04
	$[UO_2(L)Cl]$	10.11×10^{-10} $\pm 0.37 \times 10^{-10}$	2.5	3.31

1.   L. R. Avens, S. G. Bott, D. L. Clark, A. P. Sattelberger, J. G. Watkin and B. D. Zwick, *Inorg. Chem.*, 1994, **33**, 2248-2256.
2.   L. Natrajan, F. Burdet, J. Pecaut and M. Mazzanti, *J. Am. Chem. Soc.*, 2006, **128**, 7152-7153.
3.   J. M. Fritsch, K. A. Thoreson and K. McNeill, *Dalton Trans.*, 2006, 4814 - 4820.
4.   M. Stender, R. J. Wright, B. E. Eichler, J. Prust, M. M. Olmstead, H. W. Roesky and P. P. Power, *J. Chem. Soc., Dalton Trans.*, 2001, 3465-3469.
5.   J. E. Tanner, *J. Chem. Phys.*, 1970, **52**, 2523-&.
6.   D. H. Wu, A. D. Chen and C. S. Johnson, *J. Magn. Reson., Ser. A*, 1995, **115**, 260-264.
7.   C. S. Johnson, *Prog. Nucl. Magn. Reson. Spectrosc.*, 1999, **34**, 203-256.